Library Progress International
Vol.44, No.3, Jul-Dec 2024: P.113-137

Print version ISSN 0970 1052
Online version ISSN 2320 317X

Original Article

Available online at www.bpasjournals.com

Deciphering Urban Green Space using Metric Approach: A Case Study of Salt Lake and Rajarhat (Newtown)

***Abhinandan Das**

*Department of Humanities and Social Sciences, Indian Institute of Technology, Kharagpur 721302, West Bengal, India. abhinandandas24@gmail.com, abhinandandasdas2018@gmail.com, abhinandan94@iitkgp.ac.in . ORCID: https://orcid.org/0000-0003-0660-7770

How to cite this article: Abhinandan Das (2024). Deciphering Urban Green Space using Metric Approach: A Case Study of Salt Lake and Rajarhat (Newtown) 44(3), 113-137.

ABSTRACT

A specific amount of green space is significantly desirable in a densely populated urban area. During urban planning, it has been said that leaving a particular location as a green space will increase greening and, at the same time, protect the environment of the urban area. However, during urban construction, unscientific and unplanned construction of this greening is prevented. Since 2001, growth in urban construction in Kolkata's Salt Lake region has slowed the pace of greening, and this article highlights the changing spatial distribution and characteristics of UGS between 2001 and 2021. The condition of Salt Lake's UGS (Urban Green Space) has been judged through LULC (Land use land cover), LST (Land surface temperature), and NDVI (Normalized difference vegetation index). With the increase in urban construction from 2001 to 2021, LST has increased, NDVI has decreased, and urban greening has been limited to a few green patches. Currently, the condition of UGS in Salt Lake could be better, yet people are renovating several vegetated lands and wetlands to improve the environment. In the future, UGS is expected to increase in Salt Lake through plantations and with a well-timed government policy.

Keywords: Urban Green Space; Land use land cover; Land surface temperature; Normalized difference vegetation index; Urban Heat Island

1 Introduction

The term "urban green spaces" (UGS) refers to open places in cities, that are vegetated mainly by greenery and serve several purposes, both for the residents of the town and for those who travel through it (Manlun, 2003). According to Leeuwen et al. (2009), these are the most significant ecological features and, at times, eco-heritage of every given metropolis. Their size, scale, function, and location can vary, and they exhibit a wide range of natural diversity (Gill et al., 2008). The importance of parks and other green areas to city ecosystems is enormous. As greening increases in an urban area, it improves the surrounding environment as well as the mental health of the people. Many places are reserved for greening before planning any metropolitan area (Haaland & van den Bosch, 2015; Anguluri & Narayanan, 2017). Despite the valuable services they provide, urban green areas have been rapidly diminished due to the haphazard growth of cities around the world (Zhou & Wang, 2011). Kondo et al. (2018) predict that by 2050, nearly 70% of the world's population will reside in urban regions, up from over 50%. Today, along with the increase in population, the number of people from the village has also migrated to the city for various facilities, and this matter is advancing the rate of urbanization with rapid progress (Sun et al., 2013). Kim and Pauleit (2007) state that this process changes the urban environment by extending impermeable regions and reducing green space, which directly impacts on urban ecosystem. Due to increasing unplanned urbanization over time, the amount of greening in various cities of India is continuously decreasing (Xian et al., 2005; Sannigrahi et al., 2018; Yogesh et al., 2009). Prior research has primarily emphasized using subjective

methods to evaluate green spaces, which are time-consuming and costly. These techniques consist of surveys that are evaluated by professional assessors that utilize certain criteria, such as the existence or nonexistence of various characteristics, to evaluate the natural surroundings (Gupta et al., 2012; Bardhan et al., 2016). With the development of remote sensing and geographical information systems, scientists can now efficiently analyse the information obtained from a satellite image. Behavioral land-use changes can be analyzed through satellite images of the same region over time (Choudhury et al., 2019). If the land use of an urban area changes over time and is explored through satellite images, it is easy to observe the variation and declining condition of greening (Shojanoori & Shafri, 2016; Chibuike et al., 2018; Singh et al., 2018; Singh, 2018).

Reducing greenery due to construction in a particular area gradually introduced the Urban Heat Island (UHI) concept (Nieuwolt, 1966). The continuous change of LULC over time makes the issue of UHI more significant (Deosthali, 2000; Kim & Baik, 2002; Neteler, 2010). The UHI phenomenon is affected by many patterns of LULC alteration, which include modifications in vegetative cover levels, agricultural areas, and urban expansion due to factors such as building materials, spacing of homes, road construction, and the presence of railway stations. The magnitude and extent of the UHI are assessed by assessing the LST and the emissivity ratio at ground level. Sunlight is reflected directly from the ground and travels up the atmosphere as long waves radiate into the dome shape of the UHI and cause the LST. LST also changes with the change of LULC (Nichol & Hang, 2012; Miliaresis, 2016; Pramanik & Punia, 2019; Fitrahanjani et al., 2021). The phenomenon known as the UHI effect was attributed to the expansion of the urban area in conjunction with LST. LULC change in a region is mainly accelerated by dense urban construction, as emphasised by Sibanda and Ahmed (2020) and Verma et al. (2020). LST oscillates significantly due to land-use changes driven by different metropolitan area growth plans (Tafesse & Suryabhagavan, 2019; Stemn & Kumi-Boateng, 2020). While measuring surface temperature is tricky, measuring LST through satellite image bands is much easier. In UHI context, LST is utilised to classify land use through images. The data is obtained from spaceborne information's thermal infrared remote sensing (TIR) divisions. Changes in the location of UHI along a given urban area over time indicate climate change and changing land use (Hadria et al., 2019; Jain et al., 2020). As the LULC changes, so does the amount of LST, which in turn affects the location of the UHI. The temperature is very low if the number of green plants in an area is high. However, apart from NDVI, the presence of water also helps determine the temperature of a region, and the position of UHI varies significantly due to NDVI (Ghosh & Das, 2018; Ghosh et al., 2019; Asgher et al., 2021). In Southeast Asian countries, including India, extreme temperatures rise during the summer, but the temperature is much lower in areas near water. Nevertheless, examining land use patterns indicates a substantial increase in LST in regions designated for human settlement. However, temperatures around water bodies are generally lower compared to areas farther away from them, as indicated by studies conducted by Du et al. (2019), Gupta et al. (2019), and Bera et al. (2021).

The Salt Lake region, constructed between 1958 and 1965, is recognised as a meticulously designed suburban area adjacent to Kolkata. Due to its rapid urban expansion, Salt Lake, a fast-growing metropolis in India, has experienced a significant decrease in waterbodies and forestry. It has resulted in Salt Lake being referred to as a "burning stove" in recent years. Hence, examining the arrangement and makeup of UGS in Salt Lake City and evaluating the modifications in its landscape patterns can assist us in mitigating the UHI phenomenon. Nevertheless, the UGS spatial pattern has varying cooling effects in different regions (Ke et al., 2021). Therefore, additional investigation is required to enhance the impact of UGS on UHI and to elucidate the influence of UGS on UHI reduction in various cities. The analysis of the link between UGS landscape patterns and LST and NDVI in the context of changes in UGS is primarily conducted using correlation or linear regression. Moreover, the relationship between the patterns of LULC and LST differs because of variations in landscape patterns in different geographical contexts (Estoque et al., 2017; Hou & Estoque, 2020). This study investigates the spatial correlation between the patterns of green spaces and the LST and NDVI in Salt Lake City. This method uses spatial autocorrelation and spatial regression models to analyses the geographical pattern of green space across different time periods and spatial scales.

2 Materials and methods

2.1 Study area

Salt Lake emerged as part of the Bidhannagar Municipality of North 24 Parganas within a specific scientific town plan between 1958 and 1965 (located within the latitudes of 22° 36' 11" N and 22° 33' 29" N, and the longitudes of 88° 23' 43" E and 88° 26' 34" E) (Fig 1). With an area of 55.51 sq km and 218,323 people, Salt Lake is the

fourth most populous city in West Bengal. Salt Lake is known as the IT Hub of Kolkata and Northeast India. This city is known as the home of around 1500 companies and plays a vital role in the country's economic development. Also south of the Salt Lake is the presence of the East Calcutta Wetland, which is an integral part of Ramsar site conservation. Located at 11 meters above sea level, Salt Lake is divided into five polygonal shapes as city planning, further divided into 25 wards and 94 blocks. Salt Lake is surrounded by Rajarhat and Bhangar II blocks to the east, Dumdum Municipality to the west, and the northwest and KMC regions to the south. Currently, most government and business offices in West Bengal are situated in Salt Lake. Simultaneously, this region's prevalence of multi-storied houses and residences is exceedingly great. Illegally filling water bodies and damaging dams have led to the construction of urban areas resembling concrete jungles. Central Park and Eco Park are essential for maintaining the presence of green trees in the region, as they serve as the lungs of the area. This location's air pollution level is significantly higher than other areas in Kolkata. Salt Lake City, Calcutta, is typically located on a flat plain known as the Indo-Gangetic plain. High humidity levels and a tropical environment characterize the area's climate. The climate is marked by a scorching and arid summer period from March to a monsoon or rainy season from June to September, followed by a somewhat cold and excellent winter season from October to February

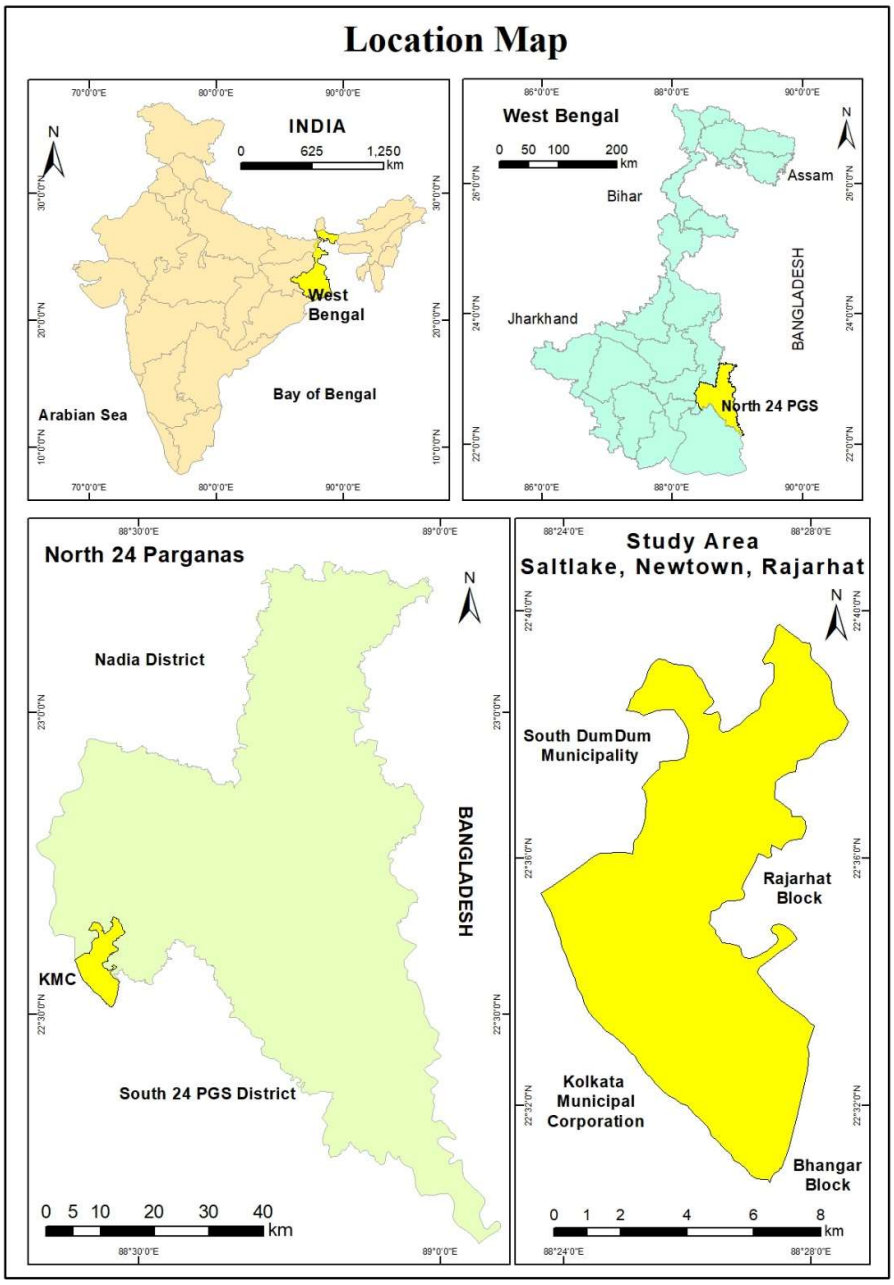

Fig. 1 Study area

2.2 Data used

2001 and 2011 LANDSAT 5 TM and 2021 LANDSAT 8 OLI satellite images were collected from Earth Explorer for LULC, NDVI and LST analysis of Salt Lake. Their accuracy has been determined in a planned way by fixing the images based on specific coordinate systems and projections. Also, several errors in the images collected from Earth Explorer have been corrected and analysed according to mathematical and radiometric methods. Also, images without clouds were collected between November and March. We did all the work through QGis and Erdas Imagine.

2.3 Methodology

2.3.1 Extraction of Land use land cover

The Landsat 5 TM satellite was utilised to capture images in 2001 and 2011, while the Landsat 8 OLI satellite was employed to capture the images in 2021. The picture classification task utilised the Support Vector Machine (SVM) supervised classification method, resulting in the extraction of six primary LULC classes (Hu et al., 2018).

The LULC classifications are obtained by categorising land into agricultural, barren, built-up areas, vegetation, water bodies, and wetlands. A validation process is carried out by digitising 400 samples from GEE to assess the accuracy of the selected LULC classes (Jia et al., 2019). The reference data is used to construct a confusion matrix. The error matrix was employed to evaluate the overall accuracy and the Kappa coefficient.

2.3.2 Analysing accuracy of LULC

The primary purpose of determining the accuracy of a satellite image is to determine how similar it is to the terrain. In the case of LULC, the accuracy of the satellite image is enhanced by how we classify it through the supervised image. An image's accuracy can be evaluated through,

$$\text{Overall Accuracy} = \text{Total number of correct samples} * 100\% \text{ total number of samples} \quad (1)$$

The authenticity of every distinction and category is determined within this investigation using a uniform formula. Zhou et al. (1998) and Lunetta et al. (2001) assert that a user's precision can be evaluated by examining metrics related to commission mistakes. The Kappa Coefficient is the primary metric for assessing accuracy (Ma & Redmond, 1995). The accuracy of three land use analyses has been assessed in this study using the Kappa coefficient. Take the detection stage (N) as an example and divide it by the diagonal frequency (∑a). After that, it speeds up at the total expected frequency (ef), split by removing all standard frequency (ef) overviews from 1. Kappa can take on values between 0 and 1, with 0 indicating a decrease in perfection and 1 representing an absolute truth. This Kappa's value is far below 0.40, indicating a lower level of accuracy in the proposal. On the other hand, according to Monserud & Leemans (1992), it is considered fair when the value is between 0.40 and 0.55, expensive when the cost is between 0.55 and 0.70, and best explained when the amount is between 0.70 and 0.85. The procedure is,

$$K = \frac{\frac{\sum a}{n} - \sum ef}{1 - \sum ef} \quad (2)$$

$$\text{Expected Frequency (ef)} = \text{row total} * \text{column total/N} \quad (3)$$

Using a change matrix, we are analyzing the alterations in LULC photographs spanning from 2001 to 2021, with a time interval of ten years (Weng, 2001). The calculations of land-use changes' gain and loss have been determined through this process.

2.3.3 Compute LST

Thermal infrared data obtained from Landsat satellite images with a spatial resolution of 100 to 120 m helps to provide information on LST (Qin et al., 2001). According to scientists, LST is determined from the infrared radiation emitted by the earth in the thermal band spectral range of 10.4 to 12.5 µm as long waves (Liu & Zhang, 2011). Three main steps typically calculate LST. First, the conversion of the digital number to spectral radiance (Lλ) can be done using the equation provided by the Landsat Project Science Office in 2002. Additionally, a new form is available for this conversion.

$$L(\lambda) = \text{gain} * DN + \text{offset} \quad (4)$$

$$L(\lambda) = \frac{LMAX - LMIN}{255} * DN + LMI \quad (5)$$

Whereas L(λ) represents the spectral radiance in W.m-2.sr-1.m-3, LMIN (1.32) and LMAX (13.67) correspond to the spectral radiance of band 6 with a DN value of 0 and 255, respectively. Furthermore, apply the methods suggested by Artis and Carnaham in 1982 to transform the spectral radiance into temperature measured in Kelvin.

$$TB = K_2/In\left(\frac{K_1}{L\lambda} + 1\right) \quad (6)$$

TB represents the brightness temperature measured by satellites, specifically LANDSAT 8 OLI and LANDSAT TM. K_1 and K_2 are calibration constants unique to these satellites' distinct bands. Finally, the conversion from kelvin to Celsius is accomplished using the following formula,

$$TB = TB - 273.15 \quad (7)$$

The equation used to determine the Land Surface Temperature (LST) for Landsat 5 TM is as follows,

$$T_s = 1/C\,[\alpha(1 - C - D) + (b(1 - C - D) + C + D)\,BT - DT_a] \quad (8)$$

Where T_s represents LST, ε denotes emissivity, and τ refers to total atmospheric emissivity. The equation for mean

atmospheric temperature is T_a=17.9769+0.9171T_0. The variables C and D are calculated using the values of ε and τ. ε is equal to 0.99 and τ is equal to 0.9. The constants α and b are adopted from Qin et al. 2001 and have values of -67.355351 and 0.458606, respectively. T_0 represents the temperature of the air near the surface. For Landsat 8 OLI, the equation used to determine the LST is as follows:

$$T_s = \frac{BT}{1 + [(\frac{\lambda BT}{\rho}) \ln \varepsilon\lambda]} \quad (9)$$

In the equation, the emitted radiance wavelength is denoted by λ, while ρ equals h (C/σ) (1.438*10-2mK). The Boltzmann constant is represented by σ, Planck's constant by h, and the velocity of light by C.

2.3.4 Calculate emissivity values

Accurate adjustment of spectral emissivity is essential for calculating LST in all geographical areas (Snyder et al., 1998). Calculations entail deriving emissivity values from NDVI measurements for every pixel. Upon implementing the required modifications, the formula now displays in the following manner,

$$\text{Land Surface Emissivity } (€) = 0.004 * Pv + 0.986 \quad (10)$$

Calculating the proportion of vegetation (Pv) in this area involves

$$Pv = \{(NDVI - NDVI_{min})/(NDVI_{max} - NDVI_{min})\}^2 \quad (11)$$

2.3.5 Spatial structure of LST

The exclusion of the wetland component from the water causes a noticeable change in the slope of each LST profile during interpolation (Gupta et al., 2019). Regarding interpolation, the weighted average is computed based on the proximity of each adjacent point. The remaining data are consolidated by integrating them, utilizing the average as the foundation. The weighted average and linear function (x_1, y_1 and x_2, y_2) are computed using data from two distinct points (Gupta et al., 2019).

$$Y = \frac{x_2 - x}{x_2 - x_1} + \frac{x - x_1}{x_2 - x_1} y_2 \quad (12)$$

$$L(X) = \frac{x_2 - x}{x_2 - x_1} + \frac{x - x_1}{x_2 - x_1} y_2 \quad (13)$$

2.3.6 Compute relation between LST and NDVI

The NDVI has been computed utilizing Landsat data to illustrate the relationship between surface temperature, area coverage, hydrological systems, and vegetation abundance. The computation of NDVI is performed using the approach described by Townshend and Justice in 1986.

$$NDVI = \frac{\text{NIR band} - \text{R band}}{\text{NIR band} + \text{R band}} \quad (14)$$

NIR is an abbreviation for the near-infrared wavelength range, whereas R denotes the red wavelength range. The computation of NDVI has been conducted utilising bands 3 and 4 for LANDSAT TM data and bands 4 and 5 for LANDSAT OLI data. NDVI is employed to signify the existence of plant life in a particular geographical area. The NDVI value spans from -1 (negative) to +1 (positive). The numbers from 0 to +1 indicate the degree of plant cover, where values closer to 1 indicate a higher density of plants (Pal & Ziaul, 2017; Choudhury et al., 2019).

2.3.7 Validation

The LST study is based on the significant changes in urban construction Salt Lake City with NDVI in 2001, 2011, and 2021 (Wu et al., 2021). The LST model was validated using the Pearson correlation matrix. Using this matrix, the LST data from 2001-2021 were compared to identify the maximum LST in the Salt Lake area.

3 Results and discussions

3.1 Changes in LULC (2001-2021)

Three decades of LULC change in Kolkata's Salt Lake region are highlighted by analysing satellite images obtained every 10-year interval from 2001 to 2021. The overall accuracy of satellite images from 2001 to 2021 is 87.21%, 88.93% and 90.23%, respectively. The kappa coefficient value also changed depending on this accuracy: 0.784, 0.729, and 0.846. According to satellite images from 2001, the presence of vegetative and agricultural land along the north and northeast of Salt Lake can be seen. At this time, bare land was in the central part, but water bodies covered the southern part. Although the presence of built-up areas is more in the western part, vegetative land and water bodies can sometimes be seen. In 2011, the built-up area increased tremendously and occupied most central, northern, eastern and western regions. Water bodies with isolated vegetative and agricultural land can only be noticed by us in the northeastern region and the central part. Due to urbanisation, much of the vegetative and agricultural land of 2001 became bare land along the western side of the area in 2011. The amount

of watershed along the south side is almost the same. In 2021, virtually all parts of Salt Lake, from the surface to the middle, have become built-up areas. Only some parts of the northeast corner and in the middle can be seen wetlands with little vegetative land. Although there is bare land in some parts of the west and wetlands in the south, the amount has decreased slightly since 2011 (Fig 2 to Fig 4).

The agricultural area in Salt Lake was 9.44 sq km in 2001, which decreased to 3.51 and 2.08 sq km in 2011 and 2021, respectively. The amount of bare land was 7.59 sq km in 2001, which increased to 14.69 sq km in 2011, and it is believed that the expansion of built-up land may have converted agricultural and vegetative land into bare land. As most of the bare land has become built-up areas in 2021, the bare land has decreased to 6.34 sq km. The built-up area has increased steadily since 2001 (9.69 sq km) and has become quite prominent in 2021 (26.70 sq km). Although the amount of vegetative land has decreased significantly from 2001 (13.84 sq km) to 2011 (3.30 sq km), in 2021, people have increased the amount of vegetative land (6.13 sq km) to improve the environment. Although the waterbody has increased slightly from 2001 (10.14 sq km) to 2011 (12.27 sq km), it has decreased somewhat in 2021 (11.70 sq km). However, the number of wetlands has continuously decreased from 2001 to 2021. While the wetlands area was five sq km in 2001, it decreased to 4.62 sq km in 2011 and 3.87 sq km in 2021 (Fig 5). Overall, reviewing the characteristics of LULC from 2001 to 2021, it can be seen that the amount of agricultural land, bare land, vegetative land and wetland decreased by 13.28%, 2.48%, 14.06% and 2.18%, respectively. However, the amount of built-up and waterbody increased by 29.6% and 2.39% respectively. It is assumed that the built-up area has increased due to excessive urbanization (Fig 6).

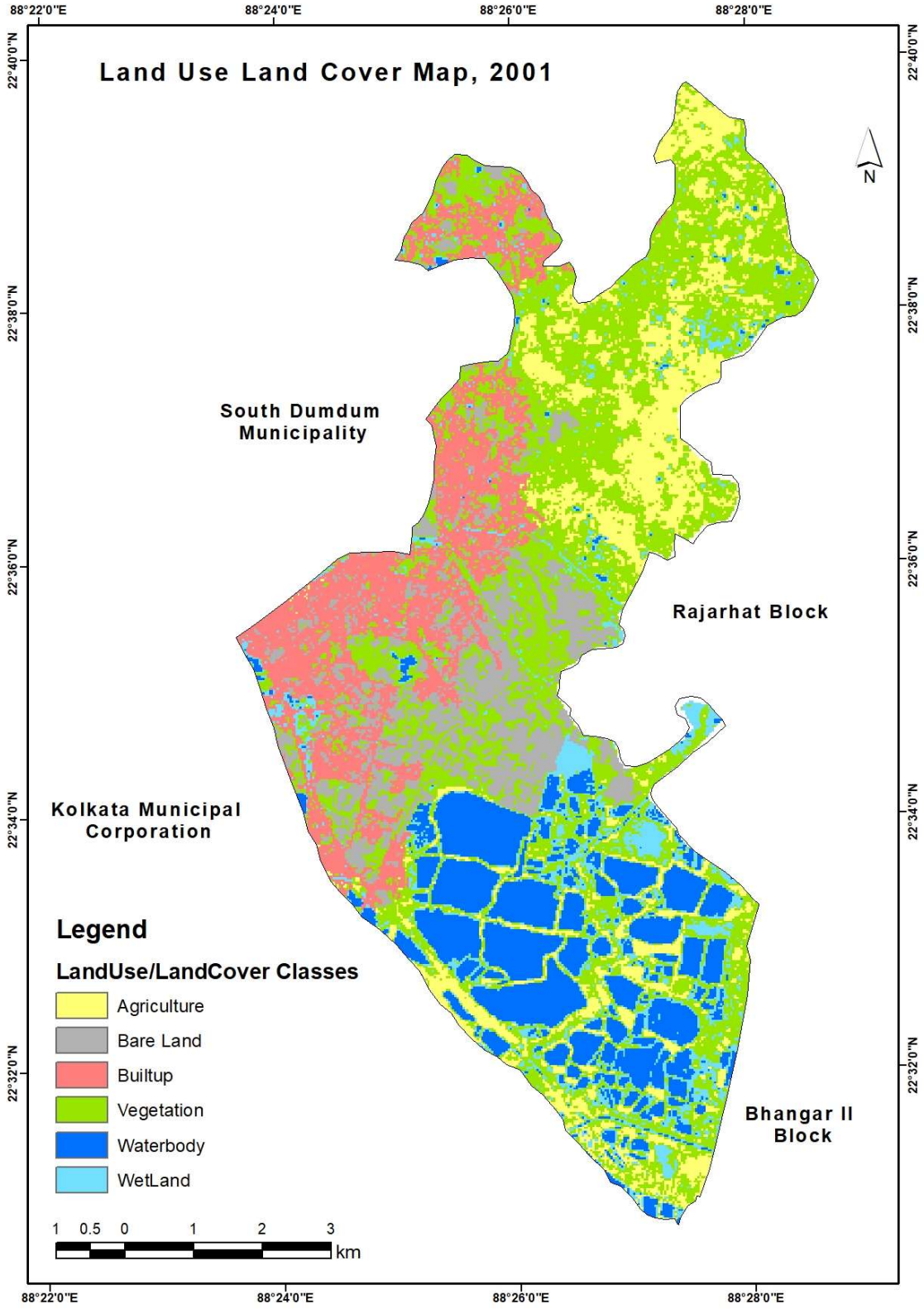

Fig. 2 Land use land cover analysis of Salt Lake, 2001

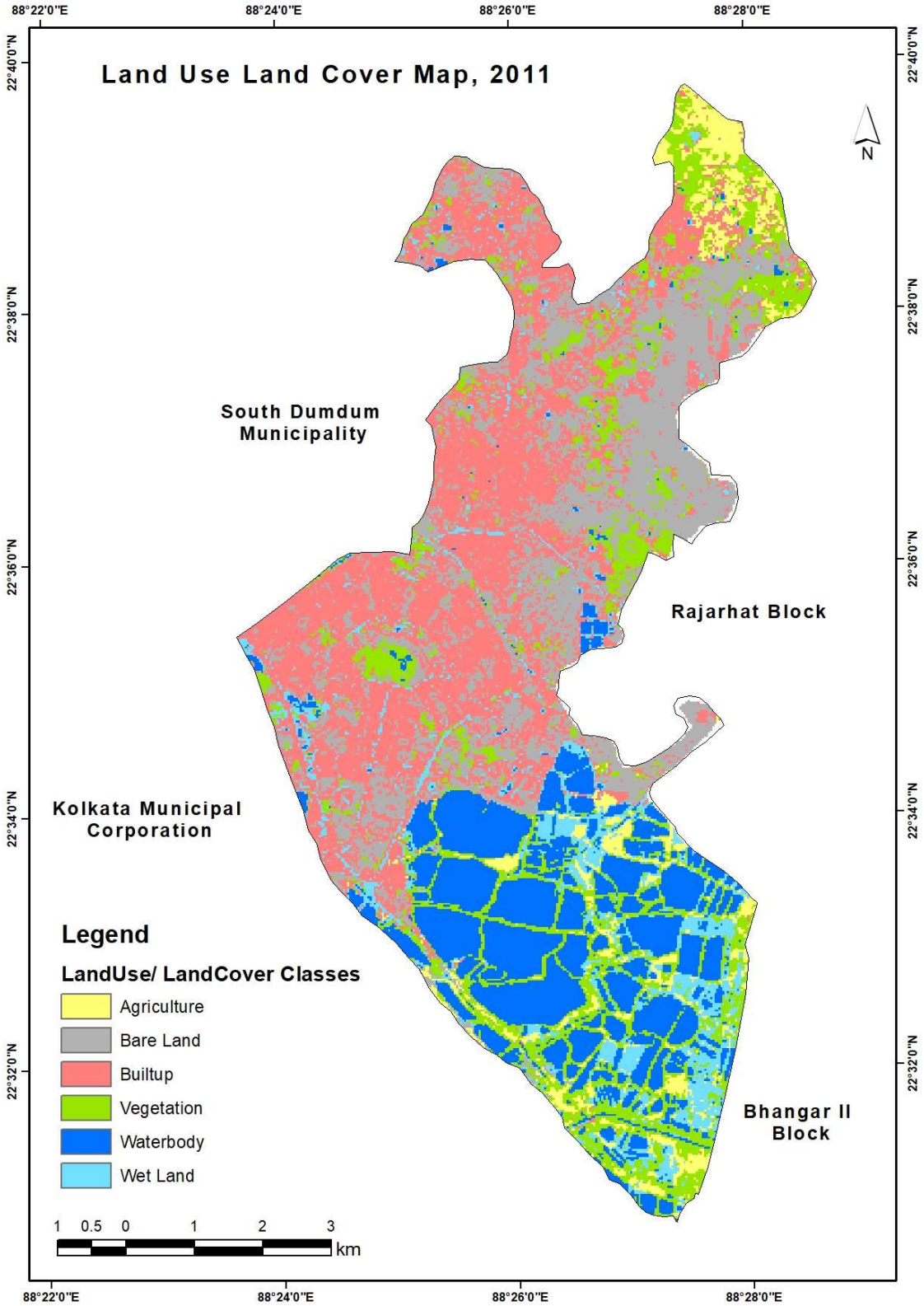

Fig. 3 Land use land cover analysis of Salt Lake, 2011

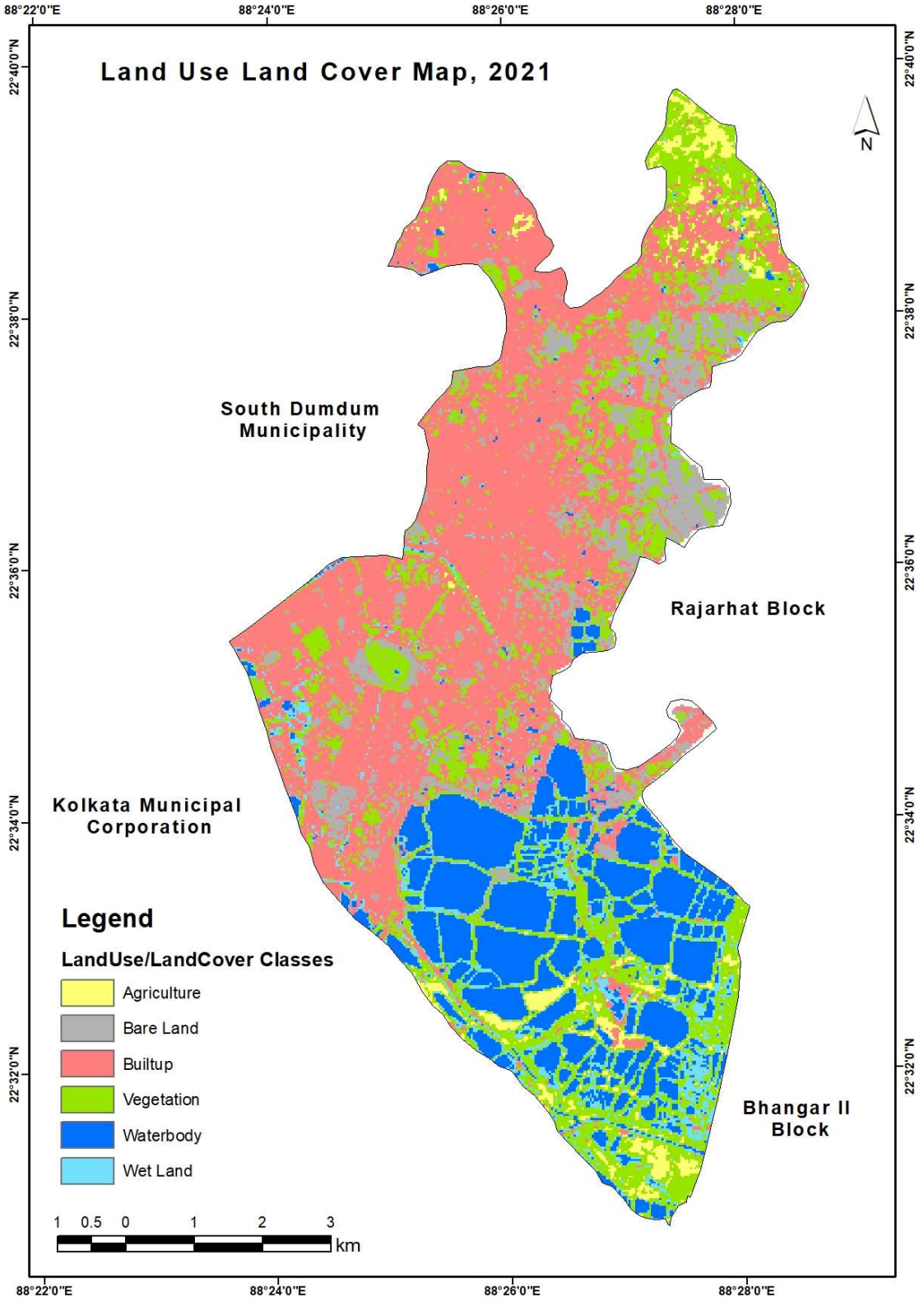

Fig. 4 Land use land cover analysis of Salt Lake, 2021

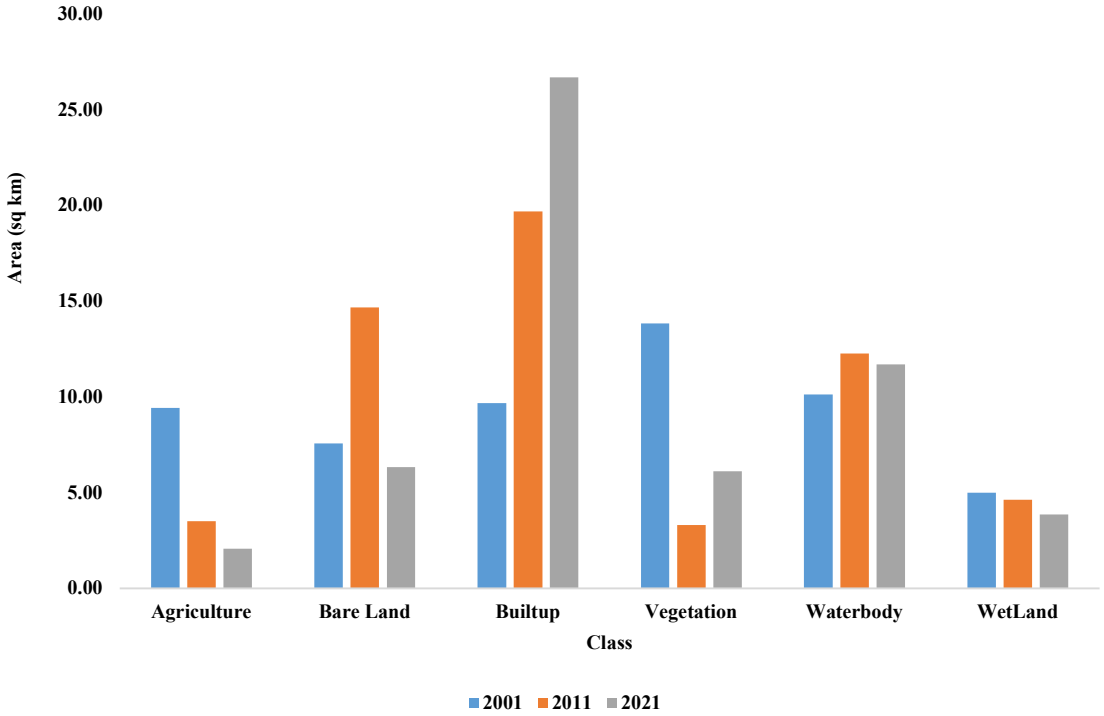

Fig. 5 Changes in land use classes of Salt Lake (2001-2021)

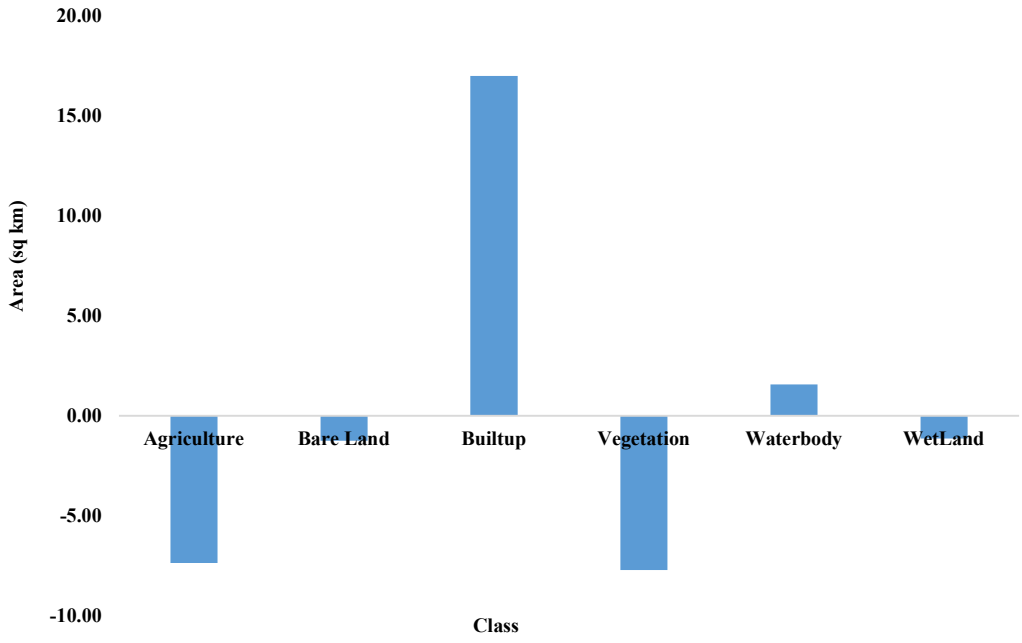

Fig. 6 Increase in built-up area of Salt Lake (2001-2021)

3.2 Changes in LST (2001-2021)

In 2001, the maximum and minimum LST in the Salt Lake region of Kolkata were 27.13^{0}c and 12.77 ^{0}c, respectively. The amount of LST is highest in the central and northwestern parts of Salt Lake due to the high volume of buildings. Again, the amount of LST is moderate due to the presence of agricultural land and wetlands in the northeastern part, eastern and western parts. However, the amount of LST could be much higher due to

abundant wetlands in the southern part. The maximum and minimum LST of Salt Lake in 2011 were 27.52 ^{0}c and 15.18 ^{0}c, respectively. The amount of LST is high enough for urbanization in the central part, northeast, northwest and some parts of the region's east side. Again, due to the agricultural land, bare land and wetlands in the north and south, the amount of LST is significantly less. The maximum and minimum LST of Salt Lake in 2021 increased to 27.93^{0}c and 14.72^{0}c, respectively. The amount of LST has increased due to the increase in the number of buildings with urbanization across the central, western, northern, northeastern and northwestern regions. However, the amount of LST could be higher due to the extensive agricultural land in the northeast corner and wetlands and wetlands in the south (Fig 7 to Fig 9).

3.3 Changes in NDVI (2001-2021)

According to the NDVI of Salt Lake in 2001, the NDVI is higher in the eastern and northeastern parts due to more agricultural and vegetative land. However, the NDVI could be higher due to the high urban construction in the central and western parts and the large number of wetlands in the south. According to the 2011 NDVI map, the NDVI is much higher due to vegetative and agricultural land along some patches in the North, East, North-East, Central and West. However, the NDVI is very low in the south, central, west and north-west parts due to the presence of water bodies and buildings. According to the 2021 NDVI map, most of the country's central, western, northwestern, eastern, and northeastern parts have low NDVI due to heavy urban construction. However, due to the presence of vegetative land along some patches in the east, northeast, south and central areas, the NDVI is higher there. In addition, the NDVI is very low due to the abundance of wetlands and fish stocks in the south. Therefore, we can see that NDVI is higher in the LULC class areas of agricultural and vegetative land from 2001 to 2021. NDVI must be higher in urban construction, bare land and wetland areas (Fig 10 to Fig 12).

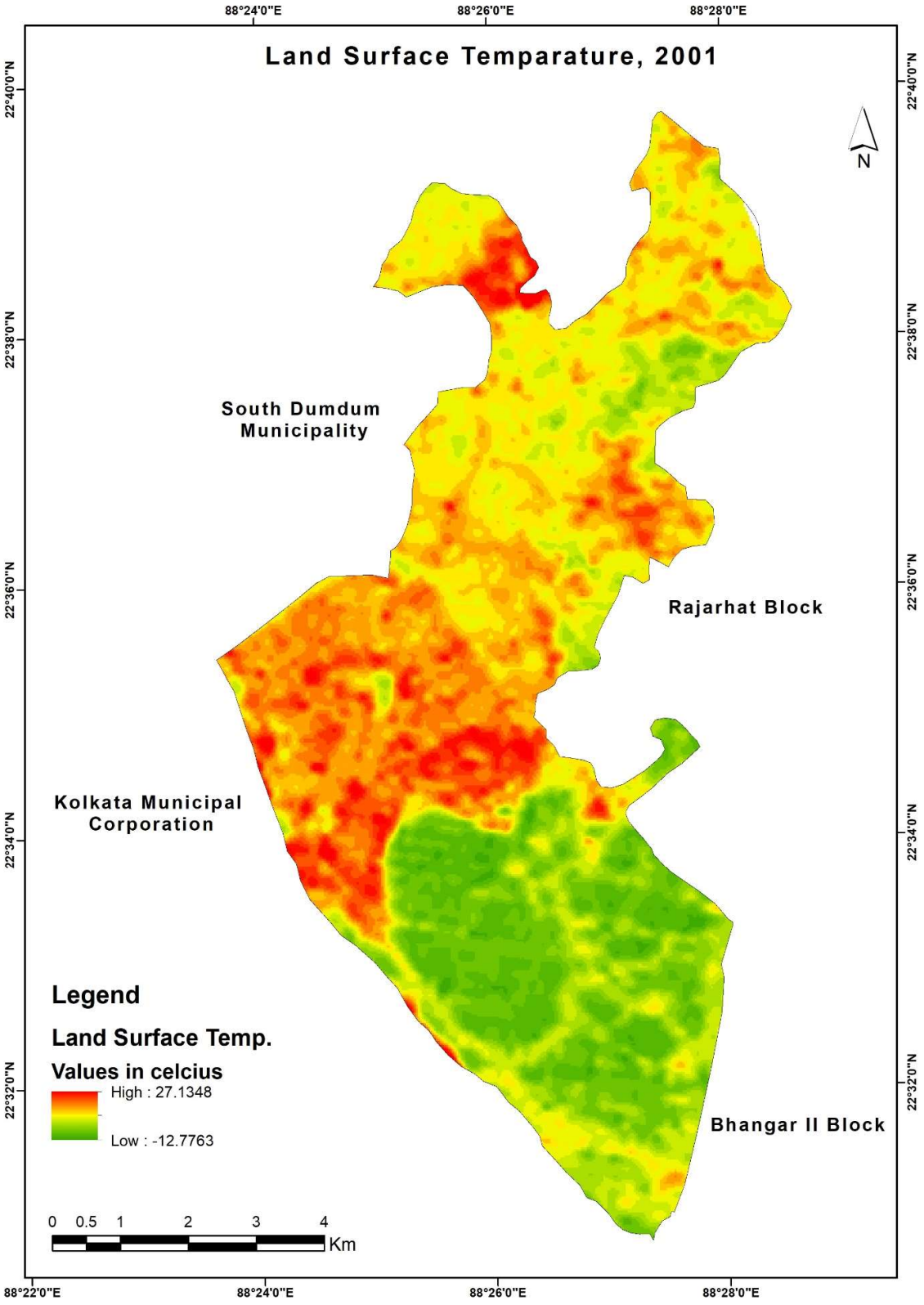

Fig. 7 Spatial distribution of LST in Salt Lake (2001)

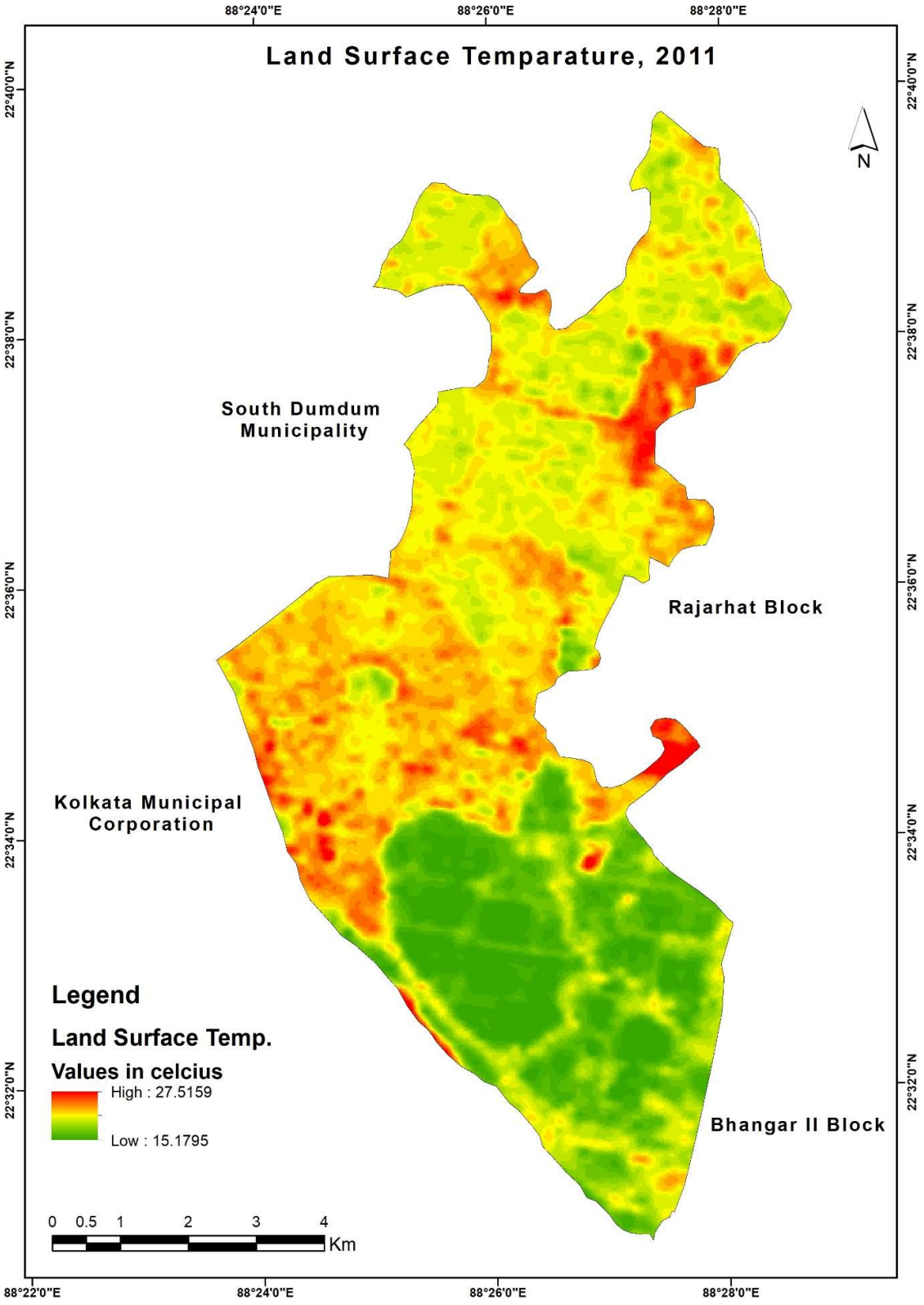

Fig. 8 Spatial distribution of LST in Salt Lake (2011)

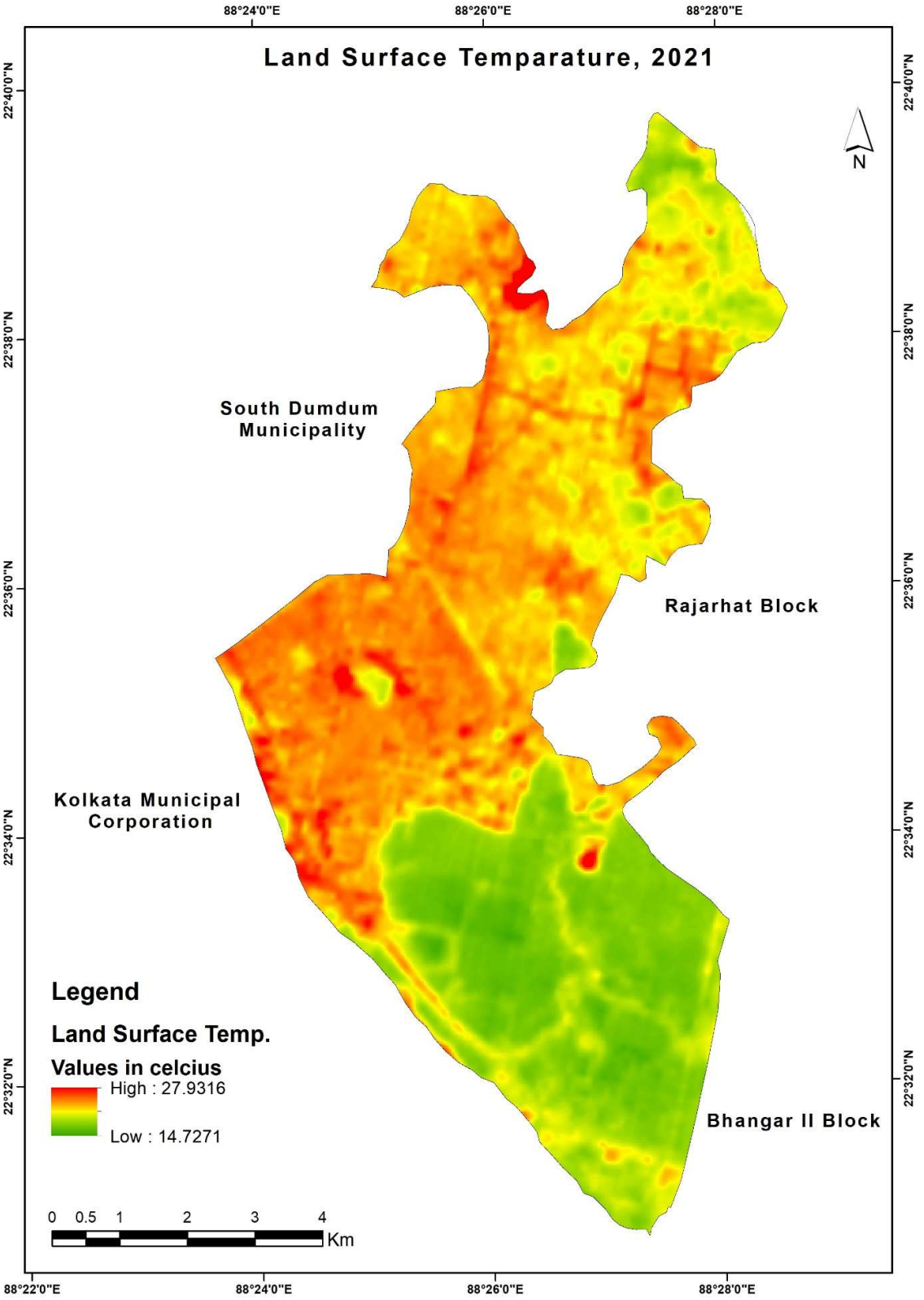

Fig. 9 Spatial distribution of LST in Salt Lake (2021)

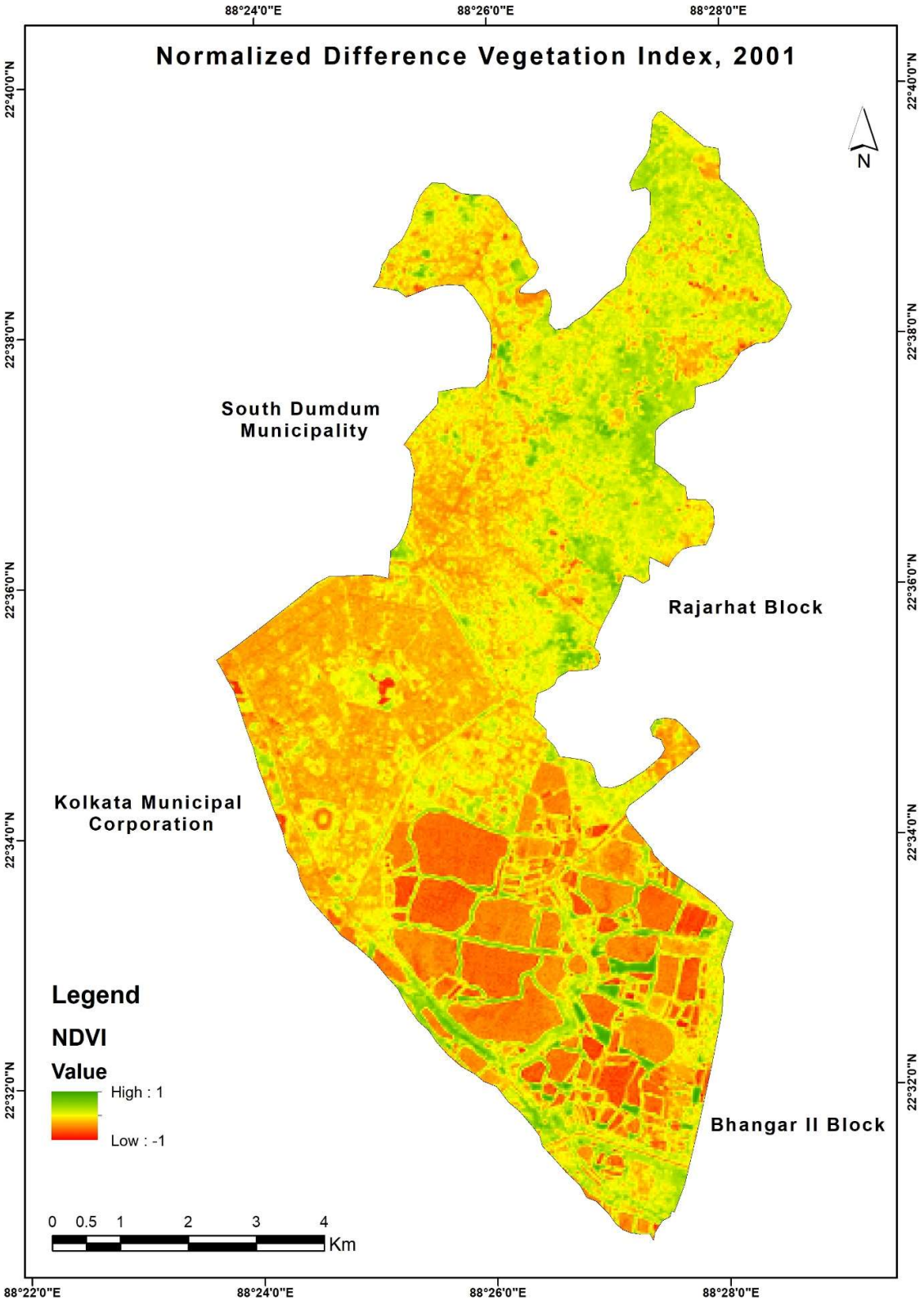

Fig. 10 Spatial distribution of NDVI in Salt Lake (2001)

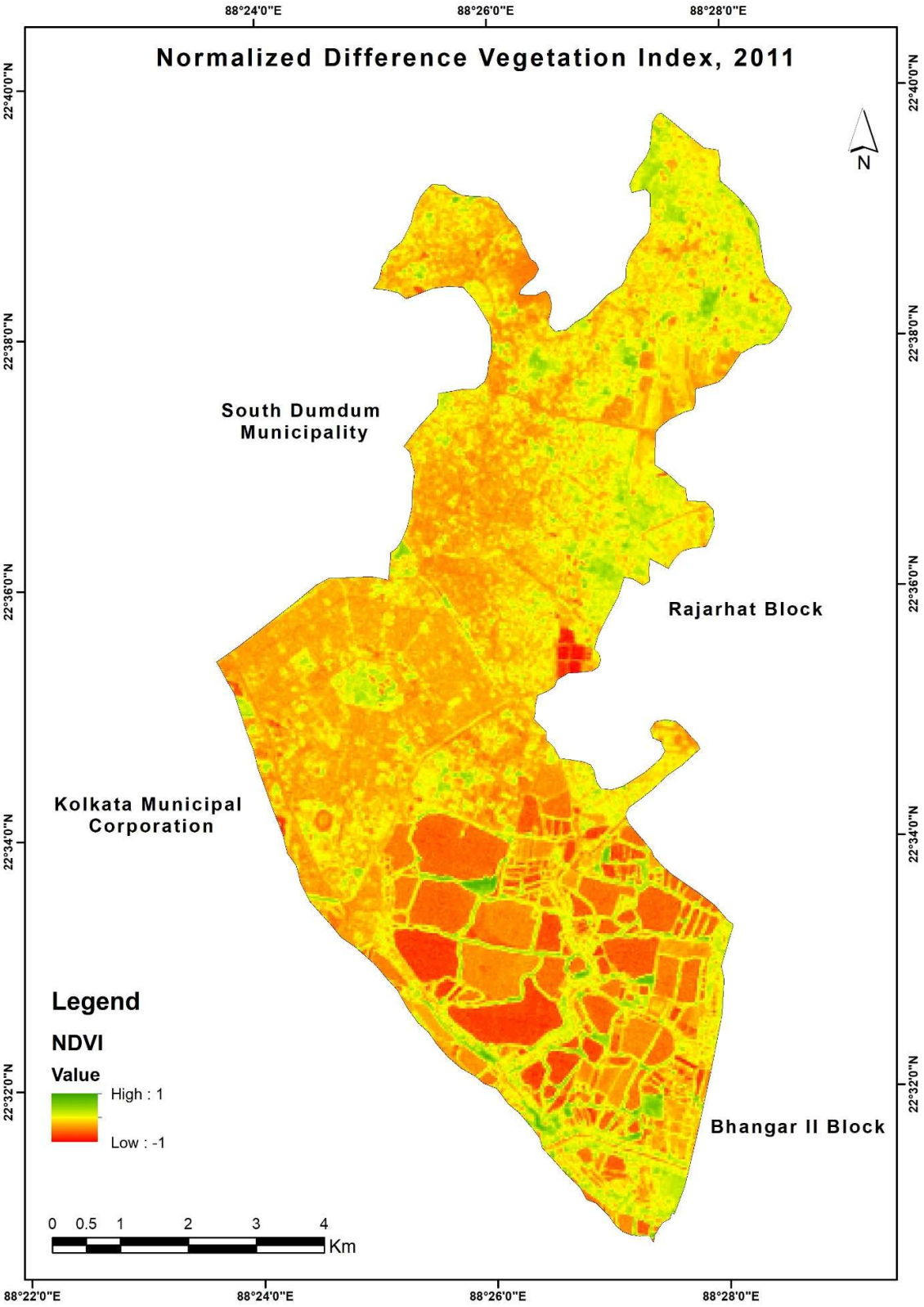

Fig. 11 Spatial distribution of NDVI in Salt Lake (2011)

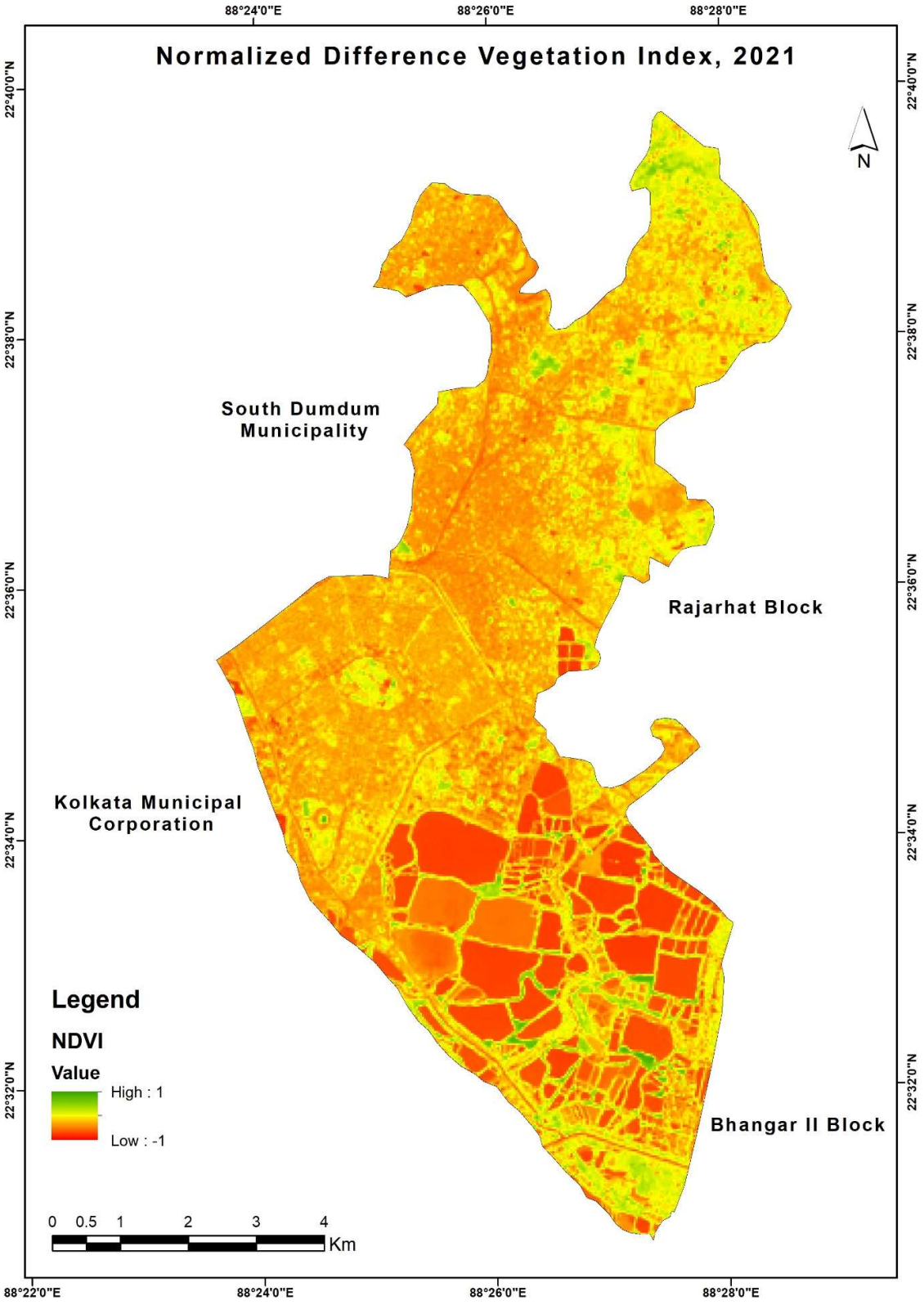

Fig. 12 Spatial distribution of NDVI in Salt Lake (2021)

3.4 Relation between changes in LULC with LST and NDVI

If the relationship of LST and NDVI with the changed LULC from 2001 to 2021 is analysed, then the concept of

UGS will be more precise. In most areas of Salt Lake, urban construction has increased since 2001, and the amount of greenery has decreased. However, in 2021, it has been seen that people have increased the amount of greening in several areas like Central Park and Eco Park to maintain the status quo of the environment. The increase in LST can be primarily prevented through increased greening. To compare LULC with LST and NDVI, we plotted the AB cross-section across the middle of the Salt Lake. The cross-section is detailed from west to east and intersects major LULC classes such as built-up areas, agricultural and vegetative land, bare land and wetlands. The total length of the cross-section is 6 km. According to the 2001 data (Fig 13), due to urban construction, the area from the west to the east of Salt Lake, about 4.25 km from the west to the east, has high LST and low NDVI. Again, after 4.25 km, LST is much lower, and NDVI is higher due to the presence of agricultural and vegetative land and wetlands. According to the 2011 data (Fig 14), the area from the west to the east of Salt Lake, up to about 4.35 km covered by urban construction, has high LST and low NDVI. Again, after 4.35 km, LST is much lower, and NDVI is higher due to the presence of agricultural and vegetative land and wetlands. According to the 2021 data (Fig 15), the area from the west to the east of Salt Lake, up to about 4.6 km, is covered by urban construction, where the amount of LST and the amount of NDVI is meagre. Again, after 4.6 km, LST is much lower, and NDVI is higher due to the presence of agricultural and vegetative land and wetlands. However, in this case, due to the building construction after 5.5 km, the amount of NDVI has decreased to some extent. Overall, it can be understood from the above analysis that LST is increasing and NDVI is decreasing due to building construction. Alternatively, the proportional relationship between LST and NDVI is responsible for UGS and LST rising as the number of greening decreases and the amount of built-up area increases.

3.5 Validation of the model

The primary tools for UGS analysis are LST and NDVI. LST increases mainly due to building construction and decreases significantly due to greening. Therefore, if the amount of NDVI increases and the amount of green space increases, the amount of LST will decrease, and the urban climate will become more stable, preventing UHI formation. The relationship between LST and NDVI changes with LULC changes is shown here through the Pearson correlation coefficient. The proportional relationship between LST and NDVI for 2001 to 2021 is shown in terms of R^2 values (Fig 16). From 2001 to 2021, if LST is low, NDVI is high, i.e. the amount of greening is increased. On the other hand, it has been seen that the amount of building construction has increased with the decrease in greening; that is, if the LST is higher, the amount of NDVI has decreased. Overall, the R^2 in this relationship is 0.867, which indicates a good relationship. Through this discussion, the amount of UGS depends on the decrease in LST.

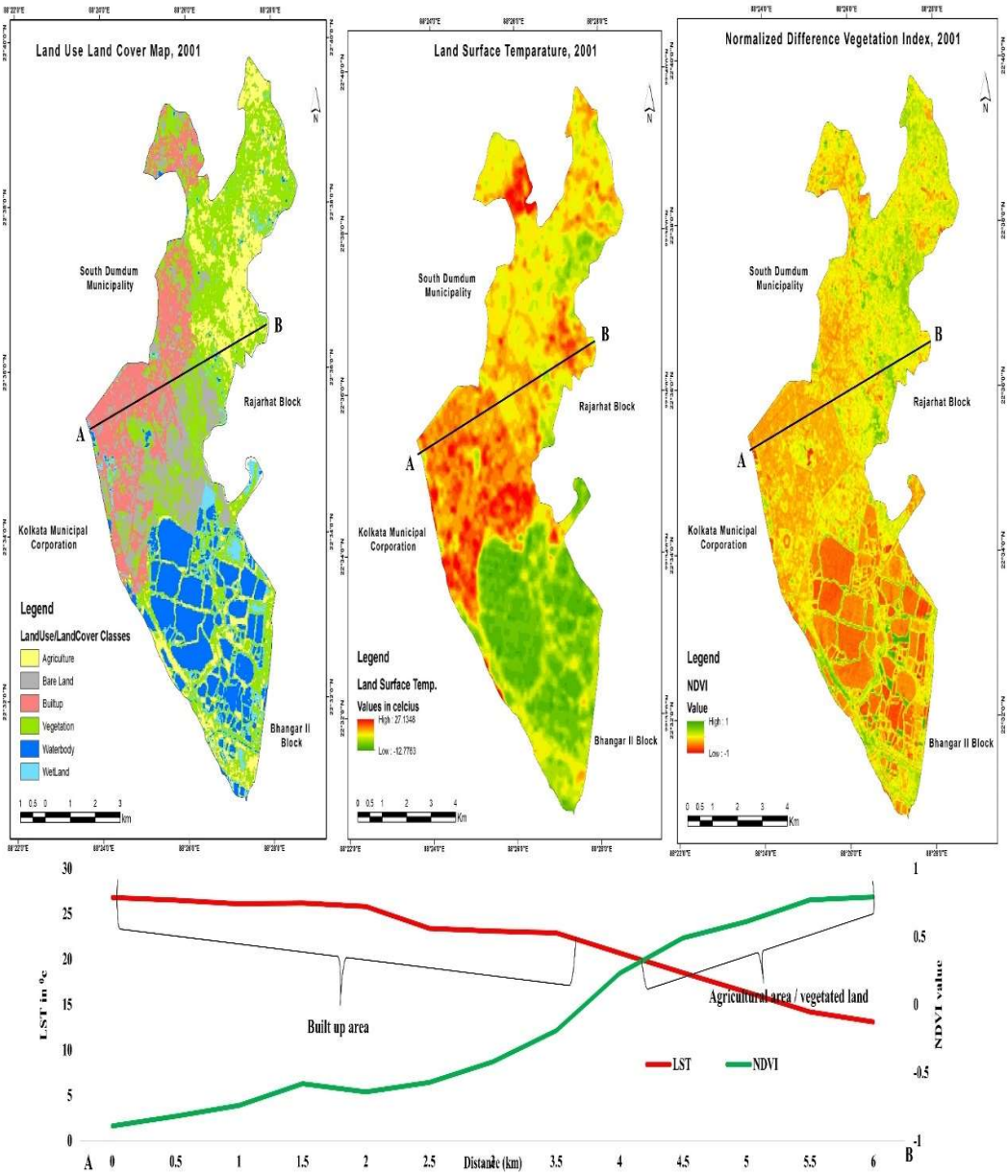

Fig. 13 Relation between LULC, LST and NDVI (2001)

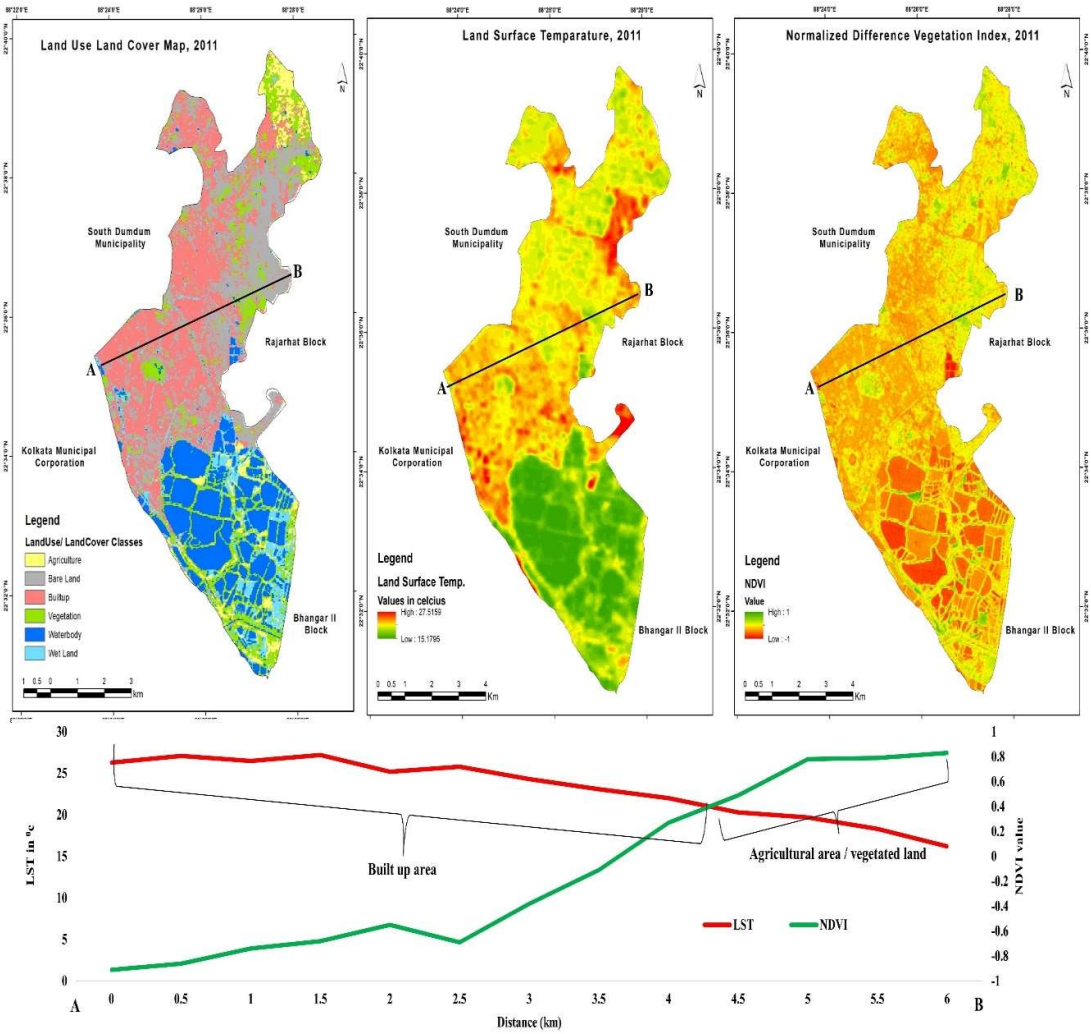

Fig. 14 Relation between LULC, LST and NDVI (2011)

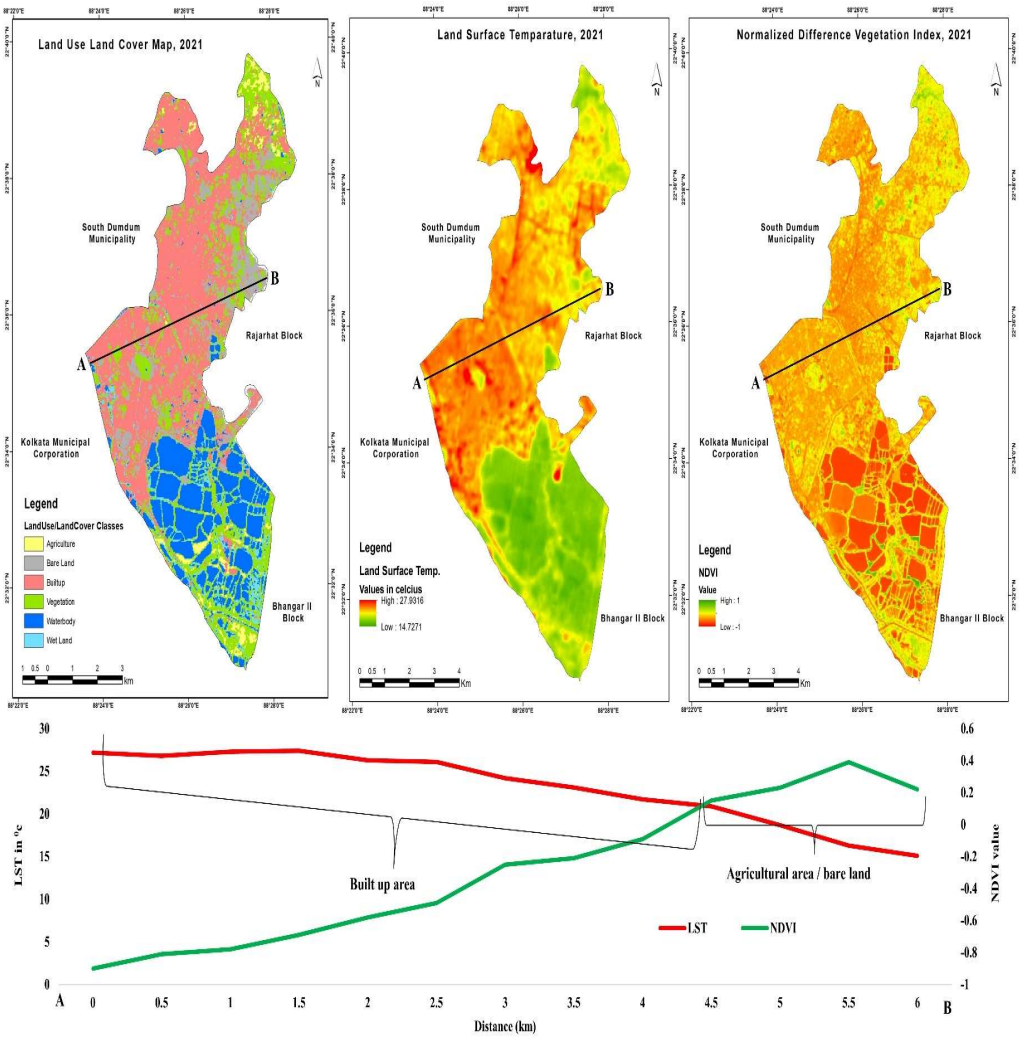

Fig. 15 Relation between LULC, LST and NDVI (2021)

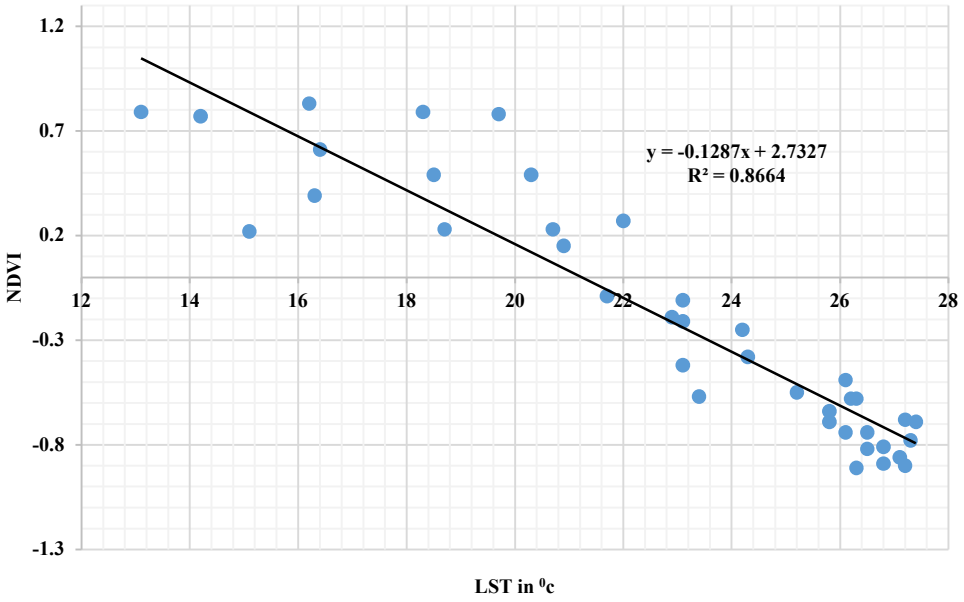

Fig. 16 Relation between LST and NDVI (2001-2021)

4 Conclusion with recommendations

Throughout the article, the changing spatial distribution and various characteristics of the urban green space of Kolkata's Salt Lake region from 2001 to 2021 have been highlighted. The Salt Lake area is a critical area of Kolkata and is known as the principal workplace of various government and private offices. Every day, many people come to this region for their work needs. Since its origin between 1956 and 1965, the area's urban construction has increased, and the amount of greening has significantly decreased. The discussion is presented based on LULC, LST, and NDVI to analyze the status of the UGS change from 2001 to 2021. From 2001 to 2021, the built-up area increased by 29.6%, but the amount of agricultural and vegetative land, bare land and wetland decreased significantly. People destroyed or destroyed them for their needs and made urban constructions there. Significantly, wetlands increased slightly during this period and may have been limited to establishing fish farms for human needs. The maximum LST in 2001 was 27.13^0c, which increased to 27.93^0c in 2021. This situation significantly highlights the increase in urban construction by destroying greenery. Although NDVI was high in agricultural and vegetative land along the northern, eastern and northeastern parts of Salt Lake in 2001, in 2021, it was limited to only a few patches. This fact shows that the amount of UGS has decreased significantly in the last 20 years, from 2001 to 2021. In the validation case, the proportional relationship of decreasing NDVI with increasing LST correctly validates the decrease in UGS.

Plantation programs are needed in a well-planned way to increase the amount of UGS. Greening alone will reduce the amount of LST and increase the amount of UGS. Above all, the Salt Lake region will be freed from the curse of UHI. However, comparing the LULC of 2011 with 2021 shows that the amount of vegetative land and wetlands in this region has increased slightly. However, humans have planned to increase the amount of vegetative land and wetlands by creating central parks, eco-parks, and fish ponds. However, in this case, the profit has been in the Salt Lake region, and it is expected that the quality of greening will shortly increase in this region through the formulation of various government plans and policies. As a result, the amount of UGS in the Salt Lake region will increase, and it can be assumed that the problem of LST and UHI will also be relieved.

5 References

Anguluri, R., & Narayanan, P. (2017). Role of green space in urban planning: Outlook towards smart cities. Urban For. Urban Green, 25, 58–65.

Artis, D.A., & Carnahan, W.H. (1982). Survey of emissivity variability in thermography of urban areas. Remote Sens Environ, 12 (4), 313–329.

Asgher, M.S., Sharma, S., Singh, R., & Singh, D. (2021). Assessing human interactions and sustainability of Wetlands in Jammu, India using Geospatial technique. Model. Earth Syst. Environ., 7, 2793–2807.

Bardhan, R., Debnath, R., & Bandopadhyay, S. (2016). A conceptual model for identifying the risk susceptibility of urban green spaces using geo-spatial techniques. Modeling Earth Systems and Environment, 2, 144.

Bera, B., Shit, P.K., Saha, S., & Bhattacharjee, S. (2021). Exploratory analysis of cooling effect of urban wetlands on Kolkata metropolitan city region, eastern India. Current Research in Environmental Sustainability, 3.

Chibuike, E. M., Ibukun, A. O., Abbas, A., & Kunda, J. (2018). Assessment of green parks cooling effect on Abuja urban micro-climate using geospatial techniques. Remote Sensing Applications: Society and Environment, 11, 11-21.

Choudhury, D., Das, K., & Das, A. (2019). Assessment of land use land cover changes and its impact on variations of land surface temperature in Asansol-Durgapur Development Region. The Egyptian Journal of Remote Sensing and Space Sciences, 22(2), 203–218.

Deosthali, V. (2000). Impact of rapid urban growth on heat and moisture islands in Pune City, India. Atmos. Environ., 34, 2745–2754.

Du, J., Song, K., & Yan, B. (2019). Impact of the Zhalong Wetland on Neighbouring Land Surface Temperatures Based on Remote Sensing and GIS. Chin. Geogra. Sci., 29(3), 1-11.

Estoque, R.C., Murayama, Y., & Myint, S.W. (2017). Effects of landscape composition and pattern on land surface temperature: An urban heat island study in the megacities of Southeast Asia. Sci. Total Environ., 577, 349–359.

Fitrahanjani, C., Prasetya, T.A.E., & Indawati, R. (2021). A statistical method for analysing temperature increase from remote sensing data with application to Spitsbergen Island. Model. Earth Syst. Environ., 7, 561–569.

Ghosh, S., & Das, A. (2018). Modelling urban cooling island impact of green space and water bodies on surface urban heat island in a continuously developing urban area. Model. Earth Syst. Environ., 4, 501–515.

Ghosh, S., Chatterjee, N.D., & Dinda, S. (2019). Relation between urban biophysical composition and dynamics

of land surface temperature in the Kolkata metropolitan area: a GIS and statistical based analysis for sustainable planning. Model. Earth Syst. Environ., 5, 307–329.
Gill, S., Handley, J. F., Ennos, A. R., Pauleit, S., Theuray, N., & Lindley, S. J. (2008). Characterising the urban environment of UK cities and towns: A template for landscape planning. Landscape and Urban Planning, 87(3), 210–222.
Gupta, K., Kumar, P., Pathan, S. K., & Sharma, K. P. (2012). Urban neighbourhood green index—A measure of green spaces in Urban Areas. Landscape and Urban Planning, 105(3), 325-335.
Gupta, N., Mathew, A., & Khandelwal, S. (2019). Analysis of cooling effect of water bodies on land surface temperature in nearby region: A case study of Ahmedabad and Chandigarh cities in India. The Egyptian Journal of Remote Sensing and Space Sciences, 22, 81-93.
Haaland, C., & van den Bosch, C. K. (2015). Challenges and strategies for urban green-space planning in cities undergoing densification: A review. Urban Forestry and Urban Greening, 14, 760–771.
Hadria, R., Benabdelouahab, T., Elmansouri, L., et al. (2019), Derivation of air temperature of agricultural areas of Morocco from remotely land surface temperature based on the updated Köppen-Geiger climate classification. Model. Earth Syst. Environ., 5, 1883–1892.
Hou, H., & Estoque, R.C. (2020). Detecting Cooling Effect of Landscape from Composition and Configuration: An Urban Heat Island Study on Hangzhou. Urban For. Urban Green., 53, 126719.
Jain, S., Roy, S.B., Panda, J., Rath, S.S. (2020). Modeling of land-use and land-cover change impact on summertime near-surface temperature variability over the Delhi–Mumbai Industrial Corridor. Model. Earth Syst. Environ., 7, 1309–1319.
Ke, X., Men, H., Zhou, T., Li, Z., & Zhu, F. (2021). Variance of the impact of urban green space on the urban heat island effect among different urban functional zones: A case study in Wuhan. Urban For. Urban Green., 62, 127159.
Kim, K. H., & Pauleit, S. (2007). Landscape character, bio diversity and land use planning: The case of Kwangju city region, South Korea. Land Use Policy, 24, 264–274.
Kim, Y.H., & Baik, J.J. (2002). Maximum Urban Heat Island Intensity in Seoul. J. Appl. Meteorol., 41, 651–653.
Kondo, M. C., Fluehr, J. M., McKeon, T., & Branas, C. C. (2018). Urban green space and its impact on human health. International Journal of Environmental Research and Public Health, 15(3), 445.
Landsat Project Science Office. (2002). Landsat 7 Science Data User's Handbook. URL: http://ltpwww.gsfc.nasa.gov/IAS/handbook/handbook_toc. html, Goddard Space Flight Center, NASA, Washington, DC (last date accessed: 10 September 2003).
Leeuwen, E. S. V., Nijkamp, P., & Vaz, T. N. (2009). The multi-functional use of urban green space. Accessed 6 June 2019.
Liu, L., & Zhang, Y. (2011). Urban heat island analysis using the Landsat TM data and Aster data: A case study in Hongkong. Remote Sens., 3, 1535-1552.
Lunetta, R.S., Iiames, J., Knight, J., Congalton, R.G., & Mace, T.H. (2001). An assessment of reference data variability using a ''virtual field reference database''. Photogramm. Eng. Remote Sens., 63, 707–715.
Ma, Z., & Redmond, R.L. (1995). Tau coefficients for accuracy assessment of classification of remote sensing data. Photogramm. Eng. Remote Sens., 61, 435–439.
Manlun, Y. (2003). Suitability analysis of urban green space system based on GIS. International Institute for Geo Information Science and Earth Observation Enschede, The Netherlands.
Miliaresis, G.C. (2016). An unstandardized selective variance reduction script for elevation, latitude, and longitude decorrelation stretches of multi-temporal LST imagery. Model. Earth Syst. Environ., 2, 41.
Monserud, R.A., & Leemans, R. (1992). Comparing global vegetation maps with the Kappa statistic. Ecol. Model., 62, 275e293.
Neteler, M. (2010). Estimating daily land surface temperatures in mountainous environments by reconstructed MODIS LST data. Remote Sens., 2, 333–351.
Nichol, J.E., & Hang, T.P. (2012). Temporal characteristics of thermal satellite images for urban heat stress and heat island mapping. ISPRS J. Photogramm. Remote Sens., 74, 153–162.
Nieuwolt, S. (1966). The Urban Microclimate of Singapore. J. Trop. Geogr., 22, 30–37.
Pal, S., & Ziaul, S. (2017). Detection of land use and land cover change and land surface temperature in English Bazar urban center. The Egypt. J. Remote Sens. Space Sci., 20 (1), 125–145.

Pramanik, S., & Punia, M. (2019). Assessment of green space cooling effects in the dense urban landscape: a case study of Delhi, India. Model. Earth Syst. Environ., 5, 867–884.

Qin, Z., Karnieli, A., & Berliner, P. (2001). A mono-window algorithm for retrieving land surface temperature from Landsat TM data and its application to the Israel-Egypt border region. Int. J. Remote Sens., 22, 3719–3746.

Sannigrahi, S., Bhatt, S., Rahmat, S., Uniyal, B., Banerjee, S., Chakraborti, S., et al. (2018). Analyzing the role of biophysical compositions in minimizing urban land surface temperature and urban heating. Urban Climate, 24, 803–819.

Shojanoori, R., & Shafri, H. Z. M. (2016). Review on the use of remote sensing for urban forest monitoring. Arboriculture and Urban Forestry, 42(6), 400–417.

Sibanda, S., & Ahmed, F. (2020). Modelling historic and future land use/land cover changes and their impact on wetland area in Shashe sub-catchment, Zimbabwe. Model. Earth Syst. Environ., 7, 57–70.

Singh, D., Mondal, S., & Hooda, R. S. (2018). Green indexing of Hisar Municipal Corporation using geospatial techniques. International Archives of the Photogrammetry, Remote Sensing and Spatial Information Sciences, XLII-5, 921–927.

Singh, K. K. (2018). Urban green space availability in Bathinda City, India. Environmental Monitoring and Assessment, 190, 671.

Snyder, W.C., Wan, Z., Zhang, Y., & Feng, Y.Z. (1998). Classification-based emissivity for land surface temperature measurement from space. Int. J. Remote Sens., 19 (14), 2753–2774.

Stemn, E., & Kumi-Boateng, B. (2020). Modelling of land surface temperature changes as a determinant of urban heat island and risk of heat-related conditions in the Wassa West Mining Area of Ghana. Model. Earth Syst. Environ., 6, 1727–1740.

Sun, C., Wu, Z., Lv, Z., Yao, N., & Wei, J. (2013). Quantifying different types of urban growth and the change dynamic in Guangzhou using multi-temporal remote sensing data. International Journal of Applied Earth Observation and Geoinformation, 21, 409–417.

Tafesse, B., & Suryabhagavan, K.V. (2019). Systematic modeling of impacts of land-use and land-cover changes on land surface temperature in Adama Zuria District, Ethiopia. Model. Earth Syst. Environ. 5: 805–817.

Townshend, J.R., & Justice, C.O. (1986). Analysis of the dynamics of African vegetation using the normalized difference vegetation index. Int. J. Remote Sens., 7 (11), 1435–1445.

Verma, P., Raghubanshi, A., Srivastava, P.K., & Raghubanshi, A.S. (2020). Appraisal of kappa-based metrics and disagreement indices of accuracy assessment for parametric and nonparametric techniques used in LULC classification and change detection. Model. Earth Syst. Environ., 6, 1045–1059.

Weng, Q. (2001). A remote sensing-GIS evaluation of urban expansion and its impact on surface temperature in the Zhujiang Delta, China. Int. J. Remote Sens., 22, 1999–2014.

Wu, Y., Xi, Y., Feng, M., & Peng, S. (2021). Wetlands Cool Land Surface Temperature in Tropical Regions but Warm in Boreal Regions. Remote Sens., 13, 1439

Xian, G., Crane, M., & Steinward, D. (2005). Dynamic modeling of Tampa Bay urban development using parallel computing. Computers & Geosciences, 31(7), 920–928

Yogesh, K., Bharath, B. D., Mallick, J., Atzberger, C., & Kerle, N. (2009). Satellite—based analysis of the role of land use: Land cover and vegetation density on surface temperature regime of Delhi, India. Journal of the Indian Society of Remote Sensing, 37(2), 201–214.

Zhou, Q., Robson, M., & Pilesjo, P. (1998). On the ground estimation of vegetation cover in Australian rangelands. Int. J. Remote Sens., 9, 1815–1820.

Zhou, W., Huang, G., & Cadenasso, M.L. (2011). Does spatial configuration matter? Understanding the effects of land cover pattern on land surface temperature in urban landscapes. Landsc. Urban Plan., 102, 54–63.